VLSI process simulation

S. A. Agamy, M. Y. Khalil, M. H. Hassan, and M. A. Abdel Raheem
Nuclear Eng. Dept., Alexandria University, Alexandria, Egypt

The task of predicting the effects of a series of process steps in the Very Large Scale Integration (VLSI) technology is extremely complex. The published literature about the commercial codes is affected by proprietary considerations, which often result in omission of many details. The aim of this work is to develop simple methodology for the simulation of the VLSI processes. This is done by considering the different models used in the simulation with all their related parameters. Thermal oxidation of silicon was modeled using the Deal-Grove model with dry or wet ambient. Using proper kinetic rate constants, the different parameters affecting oxidation process, namely, temperature, orientation, pressure, doping type and concentration, halogen additions, and traces of water could be properly simulated. Models concerned with Low Pressure CVD (LPCVD) of silicon oxide and silicon nitride were treated. Plasma etch rate for F-atom etching of Si and SiO_2, and Cl - atom etching of Si are simulated. For Cl-atom etching, pronounced crystallographic effects as well as large doping effect were characterized.

تعد عملية التنبؤ بتأثير مجموعة العمليات الداخلة في تصنيع الدوائر المتكاملة فائقة الكثافة من العمليات المعقدة. معظم برامج الحاسب المتعلقة بالموضوع تجارية وتتأثر بدرجة كبيرة بعملية التصنيع التجاري وما يترتب عليه من إغفال التفاصيل المتعلقة بعمليات التصنيع المختلفة. يهدف هذا البحث إلى عرض طريقة بسيطة لمحاكاة تصنيع هذه الدوائر. تم هذا عن طريق دراسة النماذج المختلفة لمحاكاة عمليات التصنيع مع الأخذ في الاعتبار العوامل المختلفة التي تؤثر على كل نموذج. تم محاكاة عملية الأكسدة الحرارية باستخدام نموذج ديل-جروف للأكسدة الجافة والرطبة. باستخدام المعاملات المناسبة لمعدلات التفاعل، تم محاكاة تأثير العوامل المختلفة مثل الحرارة واتجاه السطح والضغط ونوع التطعيم للسليكون وتركيزه وإضافات الهالوجينات وكذلك تأثير تركيز كميات ضئيلة من بخار الماء. تمت كذلك محاكاة الترسيب الكيميائي للسليكون على أسطح مختلفة. أما عملية النقر بواسطة البلازما فقد تمت المحاكاة لعملية النقر بواسطة الفلورين والكلور وذلك للسليكون وأكسيد السليكون. عند النقر بواسطة الكلور تم محاكاة أثر الاتجاه البللوري وكذلك النسب العالية من التطعيم.

Keywords: VLSI, Process modeling, Thermal oxidation, CVD, Plasma etching.

1. Introduction

Very Large Scale Integration (VLSI) technology consists of many steps and each step may be repeated many times while processing the integrated circuit (IC). Regardless of the different mechanisms and processes involved, these processes are done not only once but many times in a certain repetitive way according to the device under consideration. The task of predicting the effects of a series of process steps, is extremely complex. For this reason computer simulation was developed during the 1970s and now virtually all aspects of VLSI design and manufacture can be simulated [1]. VLSI process simulation is also important since new design features with higher packing densities require simulation of the process to be able to estimate results before the process is carried out.

The most widely used process modeling program, SUPREM III, had its inception at Stanford's Integrated Circuits Laboratory in 1971 with SUPREM I [2]. Since that time, many process simulation-modeling programs have been developed. Roughly speaking, there are 5 codes for one-dimensional simulation (including SUPREM), 17 codes for 2 dimensional simulation, and 2 codes for three-dimensional simulation [2]. These codes use different methods for the simulation of integrated circuits including finite element, finite difference, and finite volume as well as Monte Carlo methods [2]. In addition to research in universities, simulation programs were developed at most large semiconductor companies. It is obvious that these codes are commercial ones and in many times, their

© Faculty of Engineering , Alexandria University, Egypt

published literature is affected by proprietary considerations, which often result in omission of many details [2]. Even when any of these codes can be acquired, fundamental understanding of the different processes involved in the VLSI technology is a must for the proper and efficient use of these codes.

The aim of this work is to develop simple methodology for the simulation of the VLSI process. This is done by compiling the different models used in the simulation with all their related parameters. Putting these models in one simple computer code is an essential initial step in developing VLSI process simulation capabilities, which can only be found in commercial codes.

This work treats three processes:

(1) Thermal oxidation of silicon, where Deal-Grove model was used to determine the oxidation rates with dry or wet ambient. Dependence of oxidation rate on: (a) Temperature, (b) Pressure, (3) Crystal orientation, (4) Doping level, and (5) Role of additives was considered. The important phenomenon of enhanced oxidation rate with dry oxidation at small oxide thickness was also taken into consideration.

(2) Chemical Vapor Deposition (CVD), where models have been used for the deposition rate of epitaxial layers, polysilicon, SiO_2,and Si_3N_4 films. The effect of temperature, pressure, and doping levels were also considered.

(3) Plasma etching, where etching of Si and SiO_2 by Fluorine and Chlorine atoms as well as CF_4 + O_2 were considered. The effects of temperature, crystal orientation, doping and loading were also treated.

2. Thermal oxidation of silicon

Where thick oxides (i.e., > 0.5 μm) are desired, steam (i.e., wet oxidation) is used (≅ 1 atm or an elevated pressure of up to 25 atm). Higher pressure allows thick oxide growth to be achieved at moderate temperatures in reasonable amounts of time. Typical oxidation temperatures range from 800 to 1200 °C and should be held within ±1 °C to ensure uniformity [3]. Oxide grows at a (typical rate) of the order of 0.1 μm/h at 1000 °C in dry oxygen and at a somewhat higher rate in wet oxygen [4]. The time needed to grow a film 1 μm thick is of the order of 10 h [4].

2.1. The Deal–Grove model [5]

Deal-Grove's model for the thermal oxidation process was used in this work [5]. It is the classical model used for describing the kinetics of silicon thermal oxidation [4]. Even in the most widely used process-modeling program, SUPREM III, this model is used [2]. The model is generally valid for temperatures between 700 and 1300°C, partial pressure of 0.1-1.0 atm and oxide thickness of 300-20000 A° for both oxygen and water oxidants [5].

At steady state, rate of oxide growth is represented by the following equation [5]:

$$dX_o(t) / dt = B/(2X_o + A), \qquad (1)$$

where X_o is the total oxide thickness. It is taken to consist of two parts: an initial layer of oxide X_I that might have been present on the silicon prior to the oxidation step under consideration (typically about 20 A thick [4]), and the additional thickness grown during the oxidation step under consideration. B and B/A are the parabolic rate and the linear rate constants [3,4,6].

Eq. (1) is an essential part of the calculations. Attention is directed to have the accurate values of rate constants that depend on many parameters [7]. There is some variations of the published rate data that can not be attributed to a single cause. These variations are due to a lack of sufficient data for accurate curve fitting, existence of data in inappropriate thickness ranges, and trace impurity effects [8]. It is also important to consider rate constants to be dependent on oxide thickness [9]. This dependence was found to separate the behavior into two regimes and it will affect values of B and B/A [9]. The two regimes are [4]:

(1) An initial oxidation regime, beginning with the thin native oxide layer, in which oxidation does not follow the Deal-Grove model. Oxidation is quite rapid in that region.

(2) Beyond the initial oxidation regime, the Deal-Grove model can describe the data, and it is possible to provide physically meaningful interpretations of the coefficients of the model.

2.2. Modeling initial rapid growth of oxide film in dry thermal oxidation

Deal-Grove's simple model for thermal silicon oxidation provides excellent agreement with various normalized experimental data for both wet and dry oxidation [3]. However, the model couldn't account for thin oxide growth, since it was found that nearly an oxide film of 300 A° thickness is rapidly formed with dry oxidation. For wet oxidation, that film thickness is reduced to 25 A°.

Massoud [10, 11] have introduced a mathematical model built on analysis of experimental results by adding two new terms to the right hand side of eq. (1), accounting for the initial regime. One term for the initial phase extending to ~ 50 A° and the other for intermediate phase extending to the point of the onset of linear – parabolic model, that is:

$$dX_o(t)/dt = B/(2X_o + A) + C_1 e^{-X_o/L1} + C_2 e^{-X_o/L2}, \qquad (2)$$

where, $C_{1,2} = C^{o}_{1,2}\, e^{-\Delta EC1,2/KT}$, L is called the characteristic length. Values for C_1, C_2, L_1, L_2 are given in table 1 below.

2.3. Parametric study of dry oxidation rate

In the following section, the different parameters affecting oxidation rates will be considered. The impact of each parameter is incorporated into the oxidation rate calculations by simply modifying the linear and parabolic rate parameters, B/A and B respectively. This is shown for some parameters; namely temperature and crystal orientation; in table 1 before.

2.3.1. Temperature effects

It is known that oxide density increases, as the oxidation temperature is reduced [3]. Using the proper kinetic rate constants for the initial oxide regime and thick oxide region, oxidation rate dependence on temperature in the temperature range 900-1200 °C was calculated and is presented in fig. 1.

2.3.2. Pressure effects

At high pressures, kinetic rate-constants were found to be enhanced linearly with pressure, as shown in table 2 [12,13]. For pressures below atmospheric pressure, it was found that the same relationship still holds [12]. Fig. 2 shows the time needed to reach a

Table 1
Characteristic values for the enhancement of initial rapid thermal growth in dry oxidation process [10,11]

Temp.	Values of first term	Values of second term
T < 900 °C	C^o_1 = 0.051 μm/h (100)	C^o_2 = 39.43 * 10^7 μm/h (100)
	C^o_1 = 0.026 μm/h (111)	C^o_2 = 35.22 * 10^7 μm/h (111)
	ΔEc_1 = 0 (100)	ΔEc_2 = 2.37 eV (100)
	ΔEc_1 = 0 (111)	ΔEc_2 = 2.32 eV (111)
T > 900 °C	C^o_1 = 18.24 * 10^7 μm/h (100)	
	C^o_1 = 29.22 * 10^9 μm/h (111)	
	ΔEc_1 = 2.24 eV (100)	
	ΔEc_1 = 2.80 eV(111)	
	L_1 (100) = 7.7 * 10^{-4} μm (800 °C) = 12.4 * 10^{-4} μm (1000 °C)	L_2 = 69 * 10^{-4} μm (100)
	L_1 (111) = 10.9 * 10^{-4} μm (800 °C) = 17.1 * 10^{-4} μm (1000 °C)	L_2 = 78 * 10^{-4} μm (111)

certain oxide thickness; namely 1 μm as calculated taking into consideration the effect of pressure for (111) orientation.

2.3.3. Dependence on crystal orientation

Experiments have indicated that the oxidation kinetics is a function of the crystallographic orientation of the silicon surface [3,14]. The (B/A) constant is orientation dependent while the (B) constant is independent of orientation, since it is diffusion limited [3,14]. Taking the orientation dependence of the rate constants intro consideration, as shown in table 1, oxidation rate dependence on crystal orientation is elaborated in fig. 3 as calculated using kinetic rate constants that are orientation dependent.

2.3.4. Effects of substrate doping type and concentration

It was found that heavily doped silicon oxidizes at a faster rate than lightly doped silicon [3,6,15,16,17]. Detailed studies on boron and phosphorus doped silicon substrates have shown considerable differences in oxide growth behavior. Generally speaking, oxidation rate enhancement with boron - doped silicon is generally no greater than 20% over the undoped silicon material (i.e., intrinsic) [8]. Thus, we can roughly suggest that an increase in B for heavily doped silicon by a factor 0.2 at temperature higher than 1000°C, and no variation in B/A value as shown in table 3 below. The calculated effect of oxidation rate dependence on substrate boron-doping level is introduced in fig. 4.

Table 2
High pressure effects on kinetic rate constants for wet and dry oxidation [12, 13]. The pressure is in units of atm

Wet oxidation	Dry oxidation
$B(P,T) = B(1\ atm,T)\ P_{H_2O}$	$B(P,T) = B(1\ atm,T)\ P_{O_2}$
$B/A(P,T) = B/A(1\ atm,T)\ P_{H_2O}$	$B/A(P,T) = B/A(1\ atm,T)\ P_{O_2}^{075}$

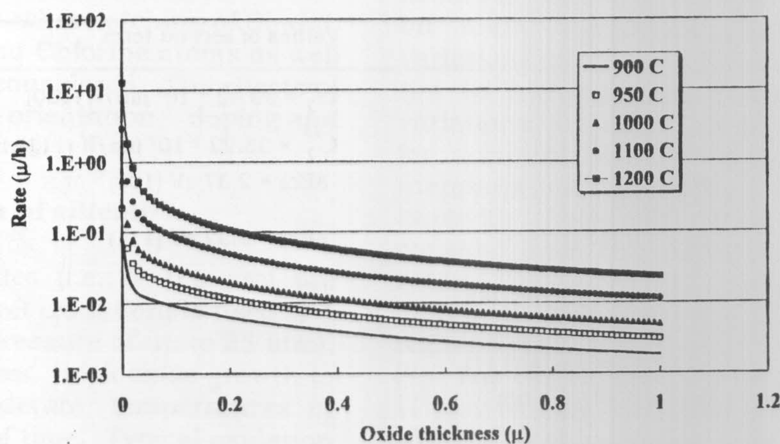

Fig. 1. Calculated oxidation dependence on temperature in the range 900-1200 C.

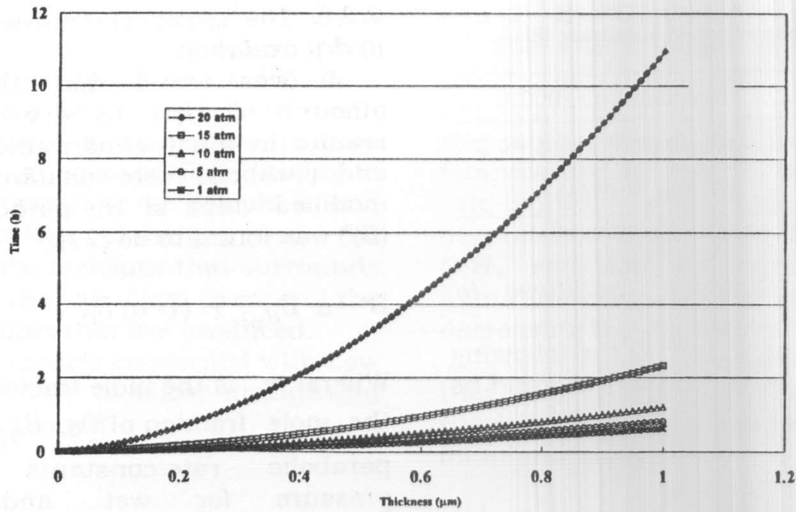

Fig. 2. Calculated time needed to grow certain oxide thickness as a function of pressure in the range 1-20 atm.

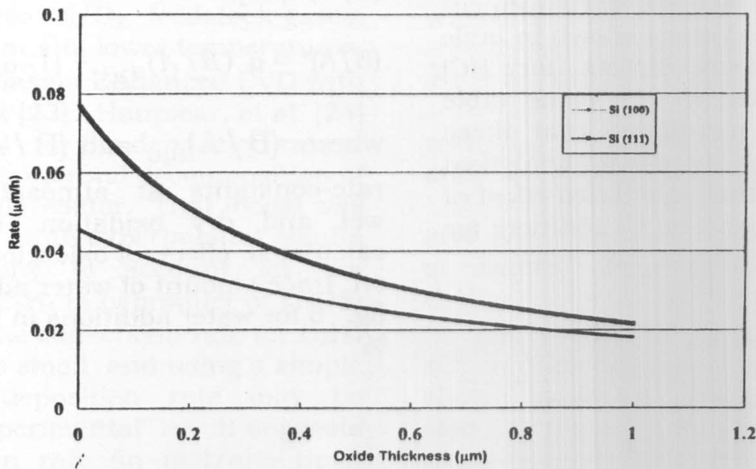

Fig. 3. Calculated oxide rate vs. oxide thickness as a function of Si orientation.

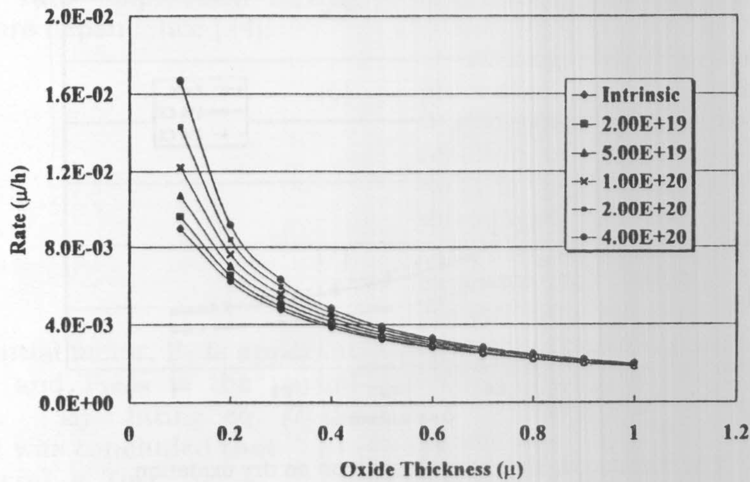

Fig. 4. Calculated rate-thickness relationship for dry oxidation of Si as a function of boron doping level.

Table 3
Enhancement factors for boron doped substrate [8]

Temperature <1000°C	Temperature >1000°C
$(B)_{Bd} = (B)_i$	$(B)_{Bd} = (B)_i *(1+f)$, f = 0.2
$(B/A)_{Bd} = (B/A)_i$	$(B/A)_{Bd} \approx (B/A)_i$

Where Bd = Boron doped, i = intrinsic material

2.3.5. The role of halogen additives to oxidation ambient

From data presented in [18] the following modifications of the rate constants could be reached,

$$B_{Cl} = B_i\,(1+f), \text{ and}$$
$$(B/A)_{Cl} = (B/A)_i\,(1+g)\,, \tag{3}$$

where i refer to the initial case of pure dry oxidation and f and g are enhancement factors, which have the values shown in table 4 below. Enhancement factors for HCl addition are also listed in the same table below. It should be mentioned that these values are simplified and there is no analytical treatment available. The calculated effect of oxidation rate-dependence on Cl addition; for 1 and 3% Cl; is shown in fig. 5.

Table 4
Enhancement factors for Cl addition

Cl concentration	B/A (g value)	B (f value)
1%	0.25	0.5
3%	0.6	0.6

2.3.6. The effect of the trace amount of water in dry oxidation

It was found that the addition of an amount of H_2O to dry oxidation ambient results in great enhancement in both linear and parabolic rate constants [19,20,21]. The modified value of the parabolic rate-constant (B)* was found to be [22]:

$$B^* = \alpha\, B_{H_2O} + (1-\alpha)\, B_{O_2}\,. \tag{4}$$

Where: α is the mole fraction of H_2O, (1- α) is the mole fraction of O_2, B_{H_2O} and B_{O_2} are the parabolic rate-constants at atmospheric pressure for wet and dry oxidation respectively. A similar equation can be written for the modefied linear rate-constant (B/A)* [22]:

$$(B/A)^* = \alpha\,(B/A)_{H_2O} + (1-\alpha)\,(B/A)_{O_2}\,, \tag{5}$$

where $(B/A)_{H_2O}$ and $(B/A)_{O_2}$ are the linear rate-constants at atmospheric pressure for wet and dry oxidation respectively. The calculated effect of oxidation rate dependence on trace amount of water addition is shown in fig. 6 for water additions in the range of 1 to 5 %.

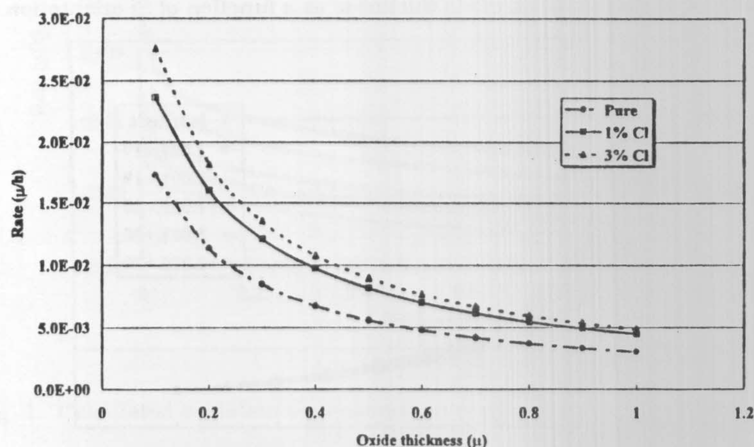

Fig. 5. Calculated effect of Cl addition on dry oxidation.

3. Chemical vapor deposition (CVD)

Chemical vapor deposition (CVD) is a technique for synthesizing materials in which chemical components in vapor phase react to form a solid film at some surface. Ability to control the components of the gas phase and the physical conditions of the gas phase, the solid surface, and the envelope that surrounds them, determines the capability to control the properties of thin films that are produced.

In this work, models concerned with Low Pressure CVD (LPCVD) of silicon dioxide and silicon nitride were treated.

3.1. CVD of SiO_2

Silicon dioxide can be deposited on substrates at 600-800 °C using SiH_4/O_2 or TEOS (tetraethoxysilane)/O_2 feedstock gases, and can be grown at still lower temperatures, 100-300 °C using Plasma Enhanced CVD with the same feedstock [23]. Haupfear, et al. [24] introduced a model for the deposition rate of SiO_2 films from the thermal decomposition of TEOS in a cold wall reactor. That model was found to fit better with experimental results and has the ability to account for the inhibition effect of C_2H_4 (a byproduct of TEOS) on growth rate. The conversion rate for C_2H_4 was found to be so small, and using a simple model for SiO_2 deposition rate may be sufficient. The experimental result suggests that overall reaction rate (in mol/area.time) can be adequately described by the following simple first order rate expression having Arrhenius temperature dependence [24]:

$$R = K_1 \; P_{TEOS} \quad . \tag{6}$$

Where,

$$K_1 = K_{10} \exp[\frac{-E_1}{RT_S}] \; . \tag{7}$$

K_{10} is a pre-exponential factor, E_1 is apparent activation energy, and P_{TEOS} is the partial pressure of TEOS. By fitting eq. (7) to experimental data, it was concluded that:
$K_{10} = 1.7 \times 10^{-3}$ mol /cm^2. s. Torr
= 27,000 μm /min.Torr
and, E_1 = 20.9 kcal/mol

The above model is valid for pressures of 0.001 to 0.1 Torr or higher and for temperatures of 750 to 950°C. The reason for the above model not to be valid at higher temperature is due to transformation of the rate-limiting step from kinetic to flux dependence [24]. Also at high pressure, the C_2H_4 emission is increased and C_2H_4 was found to compete with TEOS adsorption sites decreasing the deposition rate.

For higher pressures and temperatures that lead to high compression factor for C_2H_4, the following model can be used to account for its inhabitation effect:

$$R = \frac{K_1 P_{TEOS}}{(1 + K_2 P_{C_2H_4})^2} \, , \tag{8}$$

where,

$$K_i = K_{io} \exp[\frac{-E_i}{RT_s}] \, , \tag{9}$$

with, K_{20} = 0.00848 torr^{-1}
and, E_2 = -20.3 kcal/mol

and K_{10} , E_1, and P_{TEOS} have the same values as before. P_{C2H4} is the partial pressure of C_2H_4.

The calculated effect of TEOS pressure on silicon dioxide deposition rate at 750 °C is shown in fig. 7. Temperature dependence is also calculated in fig. 8 at a pressure of 0.005 torr.

3.2. CVD of silicon nitride

Among the commonly used LPCVD processes in semiconductor manufacture is the deposition of silicon nitride films from the reaction of ammonia (NH_3) and dichlorosilane $SiCl_2H_2$, (DCS) [25]. Roenigk and Jensen have introduced a model for silicon nitride growth rate, which was found to agree well with experimental results [26]. The following growth rate expression was found to fit better with experimental result [26]:

$$R = \frac{K_s P_{DCS} P_{NH_3}}{1 + K_1 P_{DCS} + K_2 P_{NH_3}} \; . \tag{10}$$

Where each of the above constants have Arrhenius temperature dependence and the relevant constants are given in table 5 below. P_{DCS} and P_{NH_3} are the partial pressures of DCS and NH_3 respectively. The rate expression was chosen based on preliminary fits of model predictions to the experimental data for different surface reaction mechanisms. The model is valid within 0.1- 10 torr pressure range, and 700 – 900°C temperature range.

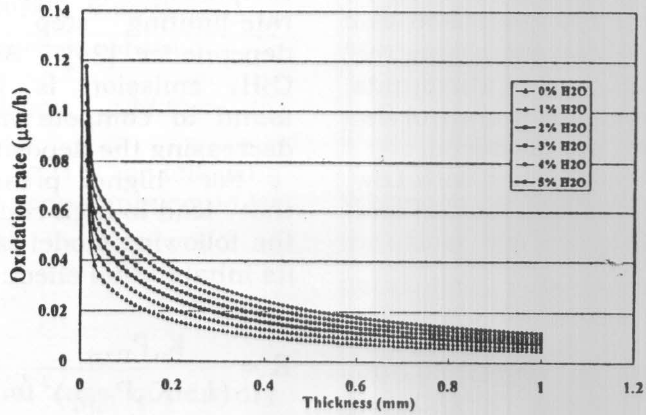

Fig. 6. Calculated effect of water additions on oxide rate thickness for dry oxidation.

Table 5
Summary of constants used in Roenigk and Jensen model for silicon nitride growth rate [26]

K_{so} (mol/m^2 - atm^2-s)	0.96×10^6
E_s * (kcal / mol)	0.83
K_{10} (atm^{-1})	4.59
E_1 (kcal/mol)	-34.82
K_{20} (atm^{-1})	0.13×10^{20}
E_2 (kcal / mol)	65.88

- Activation energies are expressed in units of kcal/mol.

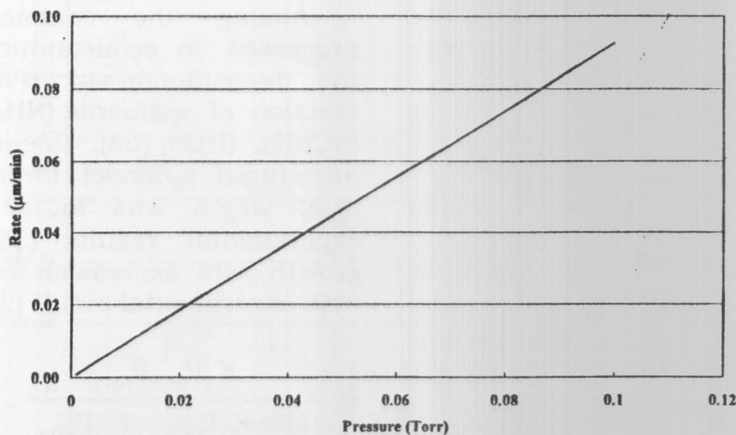

Fig. 7. Calculated effect of TEOS pressure on silicon dioxide deposition rate at 750 C.

(1) Pure chemical F-atom etching of Si and SiO_2.
(2) Pure Cl – atom etching of Si

4.1. Pure chemical F–atom etching

The etch rate have been measured to have roughly an Arrhenius form over a wide range of temperatures and to depend linearly on the gas phase of F atom density near the surface up to densities as high as 5×10^{15} cm^{-3}[23]. For undoped silicon and for thermally grown silicon dioxide, the etch rates are [23]:

$$E_{si}\ (A^\circ / min) = 2.86 \times 10^{-12}\, n_{Fs}\, T^{1/2}\, e^{-1248/T}, \quad (11)$$

$$E_{SiO2}(A^\circ/min) = 0.61 \times 10^{-12}\, n_{Fs}\, T^{1/2}\, e^{-1892/T}, \quad (12)$$

where n_{FS} (cm^{-3}) is the F-atom density near the surface and T(K) is the surface temperature. Thus, at room temperature (300 °K), and for a typical F atom density of 3×10^{14} cm^{-3}, $E_{Si} \cong 230$ A/min, $E_{SiO2} \cong 5.9$ A/min, the silicon to silicon dioxide etch rates, i.e. selectivity (S), is $\cong 40$ [23]. The Arrehnuis form of etch rate temperature dependence was also suggested by others [31,32,36].

Using eqs. 11 and 12, etch rate dependence on temperature; in °K; was calculated as shown in fig. 10 for Si and silicon dioxide. Dependence on etchants concentration (n_{Fs}), was also calculated at 400 K and shown in fig. 11.

4.2. Pure chemical Cl–atom etching

The etch rate fits a generalized Arrhenius form [23];

$$[\, E_{Si}\ (A^\circ / min) = A\, n_D\, n^{\gamma}_{cls}\, T^{1/2}\ e^{-B/T}\,], \quad (13)$$

where n^{γ}_{cls} is the surface concentration of Cl atoms and the parameters A, B, and γ are given in table 6 below. The activation energy $E_a = kB/e \approx 0.19V$ is roughly independent of the doping level and crystallographic orientation.

Table 6.
Coefficients of the modified Arehenius form for the Cl atom etching of n-type silicon [23]

Crystallographic orientation	A (A° cm $^{3+3\gamma}$ / min.$K^{1/2}$)	B (K)	γ
Polysilicon	4×10^{-18}	2365	0.39
< 100 >	1.1×10^{-17}	2139	0.29
< 111 >	1.6×10^{-31}	2084	1.03

Calculated etch rate dependence on substrate doping level (n_D) and crystal orientation for Cl atom etching at 400 °K is shown in fig. 12. This is done for n^{γ}_{cls}, i.e., chlorine atoms on the surface of 10^{13} atoms/cm^2.

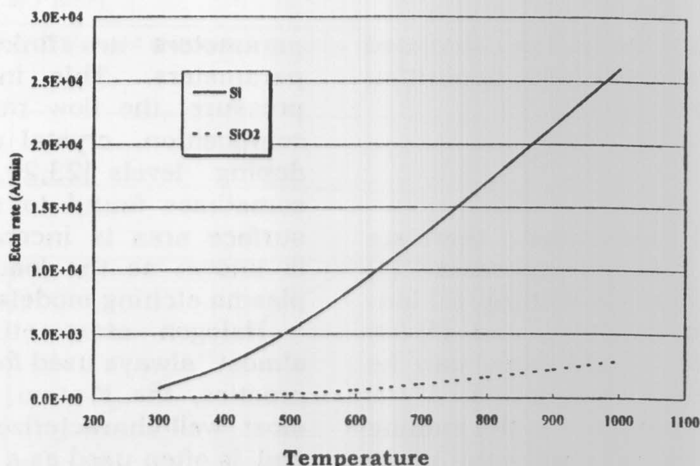

Fig. 10. Calculated etch rate dependence on temperature; in K; for silicon and silicon dioxide.

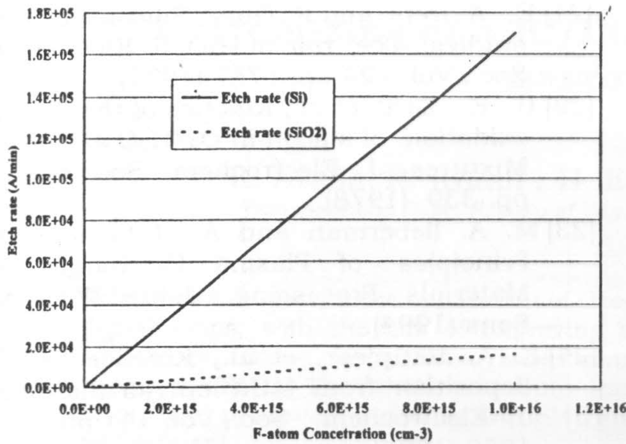

Fig. 11. Calculated etch rate dependence on etchants concentration (n_{Fs}), for silicon and silicon dioxide at 400 K.

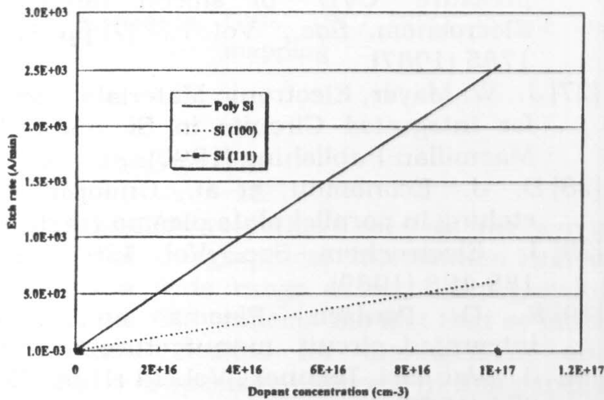

Fig. 12. Calculated etch rate dependence on substrate doping level (n_D) and crystal orientation for Cl atom etching at 400 K and chlorine atoms on the surface of 10^{13} atoms/cm^2.

5. Conclusions

(1) Deal and Grove model provides reasonable basis for thermal oxidation simulation of the VLSI.

(2) Modeling of the initial rapid oxide growth is an important phenomenon especially for the ULSI. This can be done by properly accounting for the changes in kinetic rate constants.

(3) Using proper kinetic rate constants, the different parameters affecting oxidation process, namely, temperature, orientation, pressure, doping type and concentration, halogen additions, and traces of water can be properly simulated.

(4) Many parameters involved in the etching process should be taken into account to properly account for the process. Some parameters are related to the reactor used for etching. Others are linked to the gas-surface parameters. Thus, modeling plasma-etching process suffers from the lack of many related physical constants.

(5) F-atom etching of silicon is experimentally the most well-characterized surface etch process and is often used as a paradigm for describing plasma etch processes [2].

(6) Pronounced crystallographic effects as well as large doping effect characterize chlorine atom etching.

References

[1] T. E. Price, Introduction to VLSI Technology, Prentice Hall International (1994).

[2] G. F. Carey, et al., Circuit, Device, and Process simulation, John Wiley and Sons (1996).

[3] S. M. Sze (ed.), VLSI Technology, McGraw Hill (1984).

[4] S. K. Ghandhi, VLSI Fabrication Principles, John Wiley & Sons, Inc. (1994).

[5] B. E. Deal and A. S. Grove, General relationship for the thermal oxidation of silicon, J. Appl. Phys., Vol. 36 (12) pp. 3770-3778 (1965).

[6] B. Erich, et al., Oxide growth enhancement on highly n-type doped silicon under steam oxidation, J. Electrochem. Soc., Vol. 143 pp. 1434 (1996).

[7] D. A. Antnoiadis and R. W. Dutton, Models for computer simulation of complete IC fabrication process, IEFE Trans. Solid-State Circuits, SC-14 (2) pp. 412-422 (1979).

[8] E. A. Irene and Y. J. Van der Meulen, Silicon oxidation studies: Analysis of SiO_2 film growth data, J. Electrochem. Soc., Vol. 123 (9) pp. 1380-11384 (1976).

[9] H. Z. Massoud, et al., Thermal oxidation of silicon in dry oxygen: Accurate determination of the kinetic rate

constants, J. Electrochem. Soc., Vol. 132 (7), pp. 1745-1753 (1985).

[10] Z. M. Hisham and, J. D. Plummer., Thermal-oxidation of silicon in dry oxygen growth-rate enhancement in thin regime: I. Experimental results, J. Electrochem Soc., Vol. 132 pp. 2685 (1985).

[11] Z. M. Hisham and, J. D. Plummer, Thermal-oxidation of silicon in dry oxygen growth-rate enhancement in thin regime: II. Physical mechanisms. J. Electrochem.

[12] P. C. Ho, et al., VLSI process modeling - SUPREM .III, IEEE, Trans Elect. Dev ED-30., pp. 1438 (1983).

[13] L. E. Katz and B. F. Howells, Jr., "Low temperature, high pressure steam oxidation of silicon", J. electrochem Soc. 126 (10) pp. 1822-1824 (1979).

[14] E. A. Irene, et al., "Silicon oxidation studies: Silicon orientation effects on themal oxidation", J. Electrochem. Soc., Vol. 133 (6) pp. 1253-1256 (1986).

[15] C. P. HO, and J. D. Plummer, Si/SiO_2 interface oxidation Kinetics: A physical model for the influence of high substrate doping levels: I. Theory, J. Electrochem. Soc., Vol. 126 pp. 1516 (1979).

[16] C. P. HO, and, J. D. Plummer, Si/SiO_2 interface oxidation Kinetics. A physical model for the influence of high substrate doping levels: II. Comparison with experiment and discussion," J. Electrochem. Soc., Vol. 126 pp. 1523 (1979).

[17] C. P. HO, et al., Thermal oxidation of Heavily phosphorus- Ooped silicon, J. Electrochem. Soc., Vol. 125 pp. 665 (1978).

[18] H.L. Tsai, et al., Cl incorporation at the Si/SiO_2 interface during the oxidation of silicon in HCl/O_2 ambients, J. Electrochem. Soc., Vol. 131 pp. 411 (1984).

[19] E. A. Irene, The effects of trace amount of water on the thermal oxidation of silicon in oxygen, Vol. 121 pp. 1613 (1974).

[20] D. R. Wolters and A. T. A. Zegers-van Duynhoven, On the intial regime of silicon oxidation, Phil. Mag., B 55, pp. 669 (1987).

[21] E. A. Irene and R. Ghez, Silicon oxidation studies: The role of H_2O, J. Electrochem. Soc., Vol. 124 pp. 1757 (1977).

[22] B. E. Deal, et al., Kinetics of the thermal oxidation of silicon in O_2/H_2O and O_2/Cl_2 Mixtures, J. Electrochem. Soc., Vol. 125 pp. 339 (1978).

[23] M. A. lieberman and A. J. Lichtenberg, Principles of Plasma Discharges and Materials Processing, John Wiley and Sons (1994).

[24] E. A. Haupfear, et al., Kinetics of SiO_2 deposition from tetra ethylor thosilicate, J. Electrochem. Soc., Vol. 141 pp. 1943-1950 (1994).

[25] K. S. Klaus (ed.), Handbook of Thin-Film Deposition Processes and Techniques, Noyes publications (1988).

[26] K. F. Roenigk and K. F. Jensen, Low pressure CVD of silicon nitride, J. Elecrochem. Soc., Vol. 134 (7) pp. 1777-1785 (1987).

[27] J. W. Mayer, Electronic Materials Science for Integrated Circuits in Si and GaAs, Macmillan Publishing (1990).

[28] D. J. Economou, et al., Uniformity of etching in parallel plate plasma reactors,

[29] J. Electrochem. Soc., Vol. 136 (1) pp. 188-198 (1989).

[30] R. G. Poulsen, Plasma etching in integrated circuit manufacture-A review, J. Vac. Sci. Technol., Vol. 14 (1) pp. 266-274 (1977).

[31] H. Kalter and E. P. G. T. Van de Ven, Plasma etching in IC technology, Philips tech. Rev., Vol. 38 (7/8) pp. 200-210 (1978).

[32] S. M. Sze (ed.), VLSI Technology, McGraw-Hill (1983).

[33] J.W. Coburn, Plasma Etching and Reactive ion Etching" IBM Research Laboratory Edition, (1982).

[34] S. Middleman and A. K. Hochberg, Process Engineering Analysis in Semiconductor Device Fabrication, McGraw-Hill (1993).

[35] M. Chen, et al., Etching silicon with fluorine gas, J. Electrochem. Soc., Vol. 126 (11) pp. 1946-1948 (1979).

Received: November 14, 2000
Accepted: March 19, 2001